Supporting Information

Anion-responsive Self-assembled Hydrogels of Phenylalanine-TREN Conjugate Allow Sequential Release of Propranolol and Doxorubicin

Manas Kumar Pradhan,[a] Deepika Gupta,[b] Kavthekar Rupesh Namdev,[a] Anjali,[a] Chirag Miglani,[b] Asish Pal,[*b] and Aasheesh Srivastava[*a]

Table of Contents

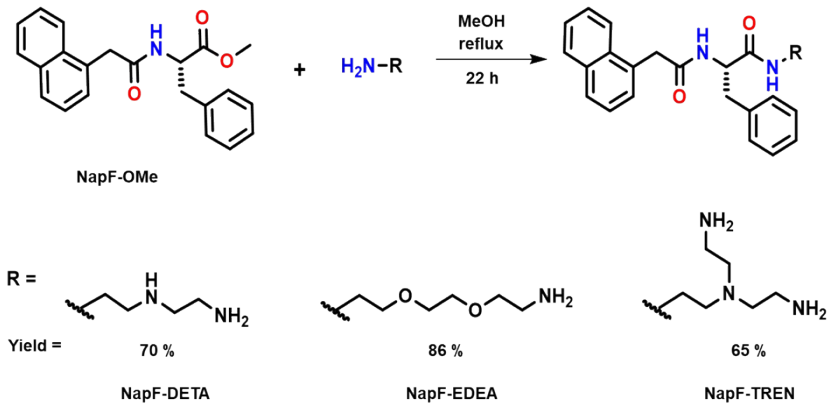

Synthetic Scheme:

Figure S1. General synthetic scheme of different NapF derivatives.

1. Synthesis and Characterization of NapF-derivative hydrogelators

1.1 Synthesis and Characterization of NapF-DETA

NapF-OMe (**1**) was used as the starting material for NapF-DETA preparation. The synthesis and characterization of NapF-OMe were reported in our previous publication[1]. Compound **1** (1 g, 1 equiv, 2.88 mmol) was taken in 10 mL of solvent methanol (sonicated and heated to dissolve). In a separate flask, Diethylenetriamine (DETA, 1.2 mL, 4 equiv, 11.52 mmol) was taken and dissolved in 3 mL of methanol. This ester solution was added dropwise to the DETA solution on stirring. Then the reaction mixture was set at 70 °C reflux. Reaction was monitored by TLC (eluent phase was 30:70 v/v EtOAc:Hex). Methanol was removed from the reaction mixture by rotary evaporator. The compound was extracted with 30 mL of $CHCl_3$ and 2 mL of bicarbonate solution (pH ~ 8) by separating funnel. The collected organic layer contained the desired product. Removal of $CHCl_3$ by rotary evaporator yielded 0.84 g (70%) of NapF-DETA as yellowish-white solid.

^{1}H NMR (500 MHz, $CDCl_3$, ppm): δ 2.40-2.50 (4H, NH-CH_2), 2.58-2.63 (2H, Phe-CH_2), 2.67-2.89 (3H, NH, NH_2-CH_2), 3.04-3.14 (2H, NH- CH_2), 3.86-3.96 (2H, Nap- CH_2), 4.46-4.54 (1H, NH-CH), 5.95-5.97 (1H, NH), 6.22 (1H, NH), 6.76-7.08 (5H, Phe CH), 7.25-7.85 (7H, Nap CH). HRMS (ESI): $C_{25}H_{30}N_4O_2$+H^+ calc.: 419.24, found: 419.24.

1.2 Synthesis and Characterization of NapF-EDEA

Compound **1** (1 g, 1 equiv, 2.88 mmol) was taken in 10 mL of methanol (sonicated and heated to dissolve). In a separate flask, 2,2′-(ethylenedioxy)-bis-(ethylamine) (EDEA, 1.680 mL, 4 equiv, 11.52 mmol) was dissolved in 3 mL of methanol. The ester solution was added dropwise to the EDEA solution with stirring. Then the reaction mixture was set at 70 °C reflux. Reaction was monitored by

TLC (eluent phase was 30:70 v/v EtOAc:Hex). Methanol was removed from the reaction mixture by rotary evaporation. The compound was extracted with 30 mL of $CHCl_3$ and 2 mL of bicarbonate solution (pH ~ 8) by separating funnel. The collected organic layer contains the desired product. Removal of $CHCl_3$ by rotary evaporator yielded 1.14 g (86%) of NapF-EDEA as yellowish-white solid.

^{1}H NMR (500 MHz, $CDCl_3$, ppm): δ 2.72-2.82 (4H, NH_2-CH_2, NH_2), 3.18-3.32 (4H, Phe-CH_2, NH-CH_2), 3.34-3.50 (8H, O-CH_2), 3.86-3.96 (2H, Nap- CH_2), 4.54-4.59 (1H, NH-CH), 6.06-6.12 (1H, NH), 6.69 (1H, NH), 6.75-7.05 (5H, Phe CH), 7.24-7.84 (7H, Nap CH). HRMS (ESI): $C_{25}H_{30}N_4O_2$+H^+ calc.: 464.25, found: 464.25.

1.3 Synthesis and Characterization of NapF-TREN

Compound **1** (1 g, 1 equiv, 2.88 mmol) was taken in 10 mL of solvent methanol (sonicated and heated it to dissolve). In a separate flask, Tris(2-aminoethyl)amine (TREN, 1.720 mL, 4 equiv, 11.52 mmol) was dissolved in 3 mL of methanol. The ester solution was added dropwise to the amine solution with stirring. Then the reaction mixture was set for reflux at 70 °C. Reaction was monitored by TLC (eluent phase was 30:70 v/v EtOAc:Hex). Methanol was removed from the reaction mixture by rotary evaporation. The compound was extracted with 30 mL of $CHCl_3$ and 2 mL of bicarbonate solution (pH ~ 8) by separating funnel. The collected organic layer contains the desired product. Removal of $CHCl_3$ by rotary evaporator yielded 0.8 g (65%) of NapF-TREN as white solid.

^{1}H NMR (500 MHz, $CDCl_3$, ppm): δ 2.30-2.38 (6H, N-CH2), 2.44 (2H, Phe-CH_2), 2.49-2.57 (4H, NH_2), 2.67-2.83 (4H, NH_2-CH_2), 2.96-3.22 (2H, NH- CH_2), 3.86-3.96 (2H, Nap- CH_2), 4.54-4.59 (1H, NH-CH), 6.23-6.25 (1H, NH), 6.75-7.05 (5H, Phe CH), 7.25-7.85 (8H, Nap CH, and NH). HRMS (ESI): $C_{27}H_{35}N_5O_2$+H^+ calc.: 462.28, found: 462.28.

2. Self-assembly study of NapF-derivative hydrogelators

2.1 CAC calculation

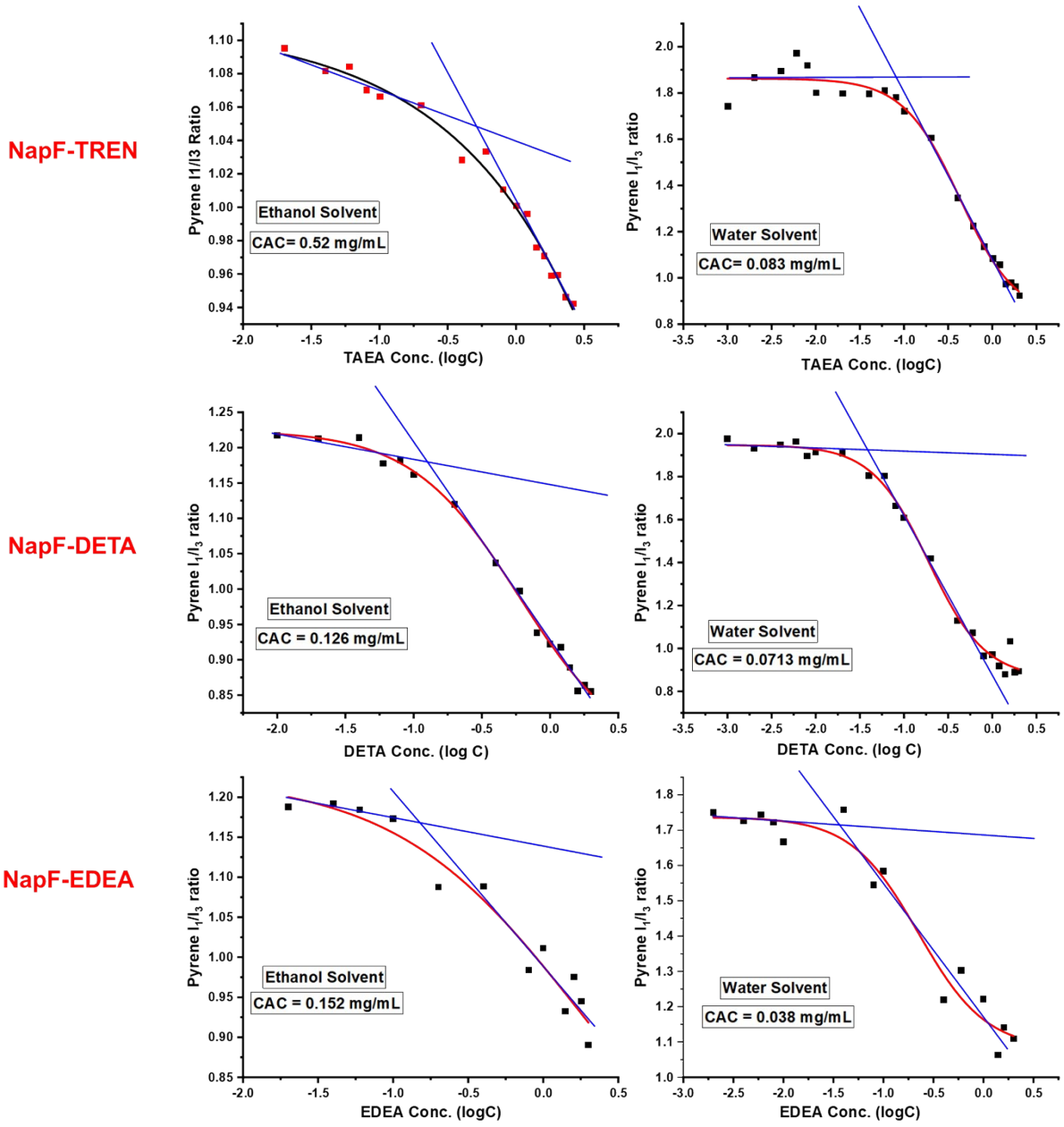

Figure S2. Critical Aggregation Concentration (CAC) of NapF-derivatives in ethanol and water solvent. I_1/I_3 ratio of pyrene fluorescence is plotted against conc. of NapF-derivative.

Table S1. Critical Aggregation Concentration (CAC) values of NapF-derivatives in ethanol and water.

Gelators	CAC (mg/mL, in EtOH)	CAC (mg/mL, in Water)
NapF-TREN	0.52	0.083
NapF-DETA	0.126	0.071
NapF-EDEA	0.152	0.038

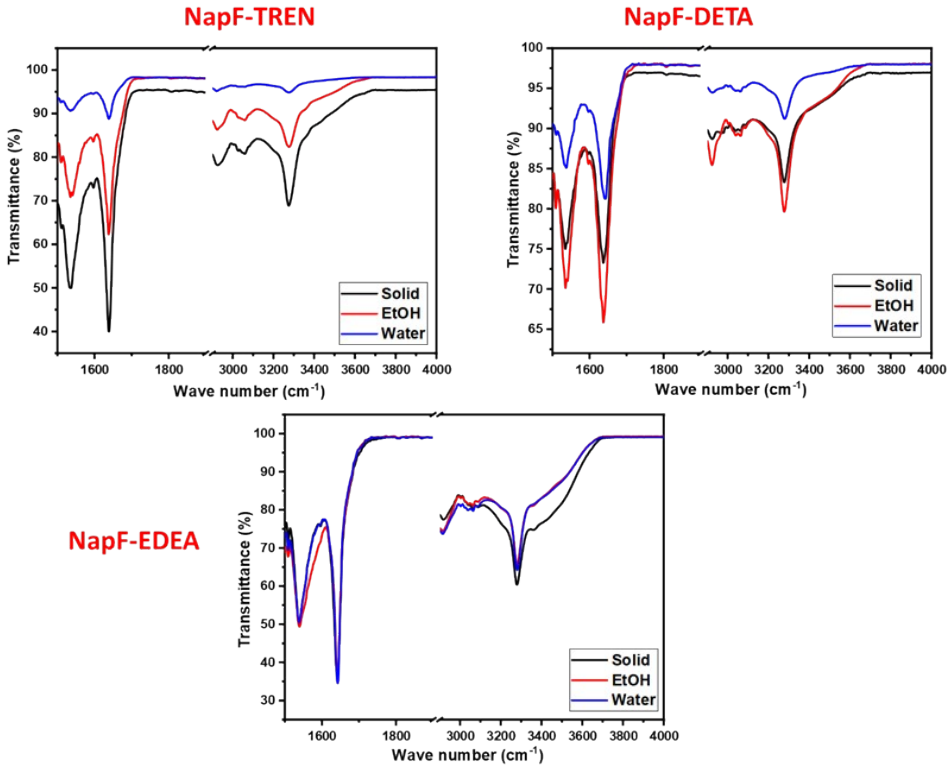

2.2 FT-IR study

Figure S3. FT-IR spectra of NapF-derivatives in the solid state in ATR mode. As prepared compounds (black profiles), vacuum-dried samples from ethanolic solutions (red profiles) and vacuum-dried self-assemblies from water (1 mg/ml, blue profiles).

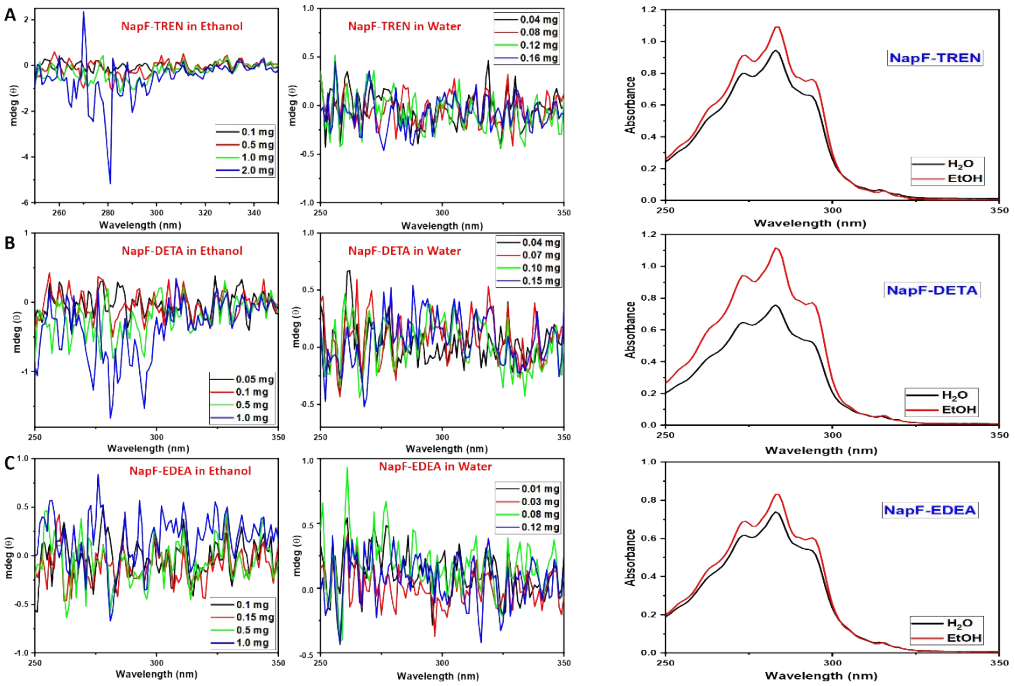

2.3 Circular Dichroism study and UV-Vis absorbance study

Figure S4. CD spectra of NapF-derivatives at CAC values in ethanol and water (left panels). UV-Vis spectra of NapF-derivatives at 0.1 mg/mL concentration in ethanol and water (right panels).

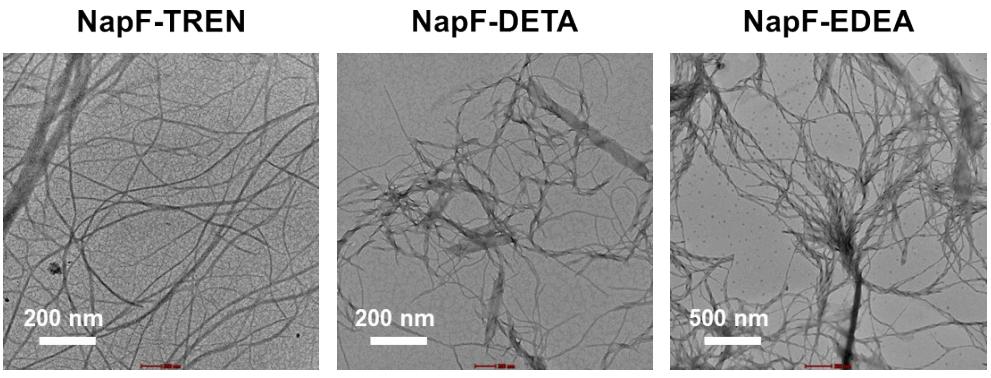

3. TEM study of NapF-derivatives self-assembly

Figure S5. TEM images of NapF-derivatives at 1 mg/mL in deionized water. The sample solutions were drop-cast on copper grid followed by vaccum drying for 12 h. Phosphotungstic acid (PTA) was used as a staining agent for contrast enhancement.

4. Anion screening of NapF hydrogels

Figure S6. Anion screening of hydrogels. **A)** NapF-TREN (10 mg, 22 mM), **B)** NapF-DETA (10 mg, 24 mM), and **C)** NapF-EDEA (10 mg, 22 mM) in presence of sub-stoichiometric concentration (6.5 mM, 0.3 equiv.) of different anions viz. 1. Control (pristine gel), 2. Cl^-, 3. $H_2PO_4^-$, 4. HPO_4^{2-}, 5. CO_3^{2-}, 6. HCO_3^-, 7. SO_4^{2-}, 8. HSO_4^-. The red ovals indicate the partial disruption of the hydrogel in presence of $H_2PO_4^-$, and HSO_4^-.

Figure S7. Anion responsive disruption of deuterogels of NapF-TREN (22 mM in D_2O) in presence of different anions (32 mM, 1.5 equiv.) *viz*. vial marking 1. Control (pristine gel), 3. $H_2PO_4^-$, 8. HSO_4^- anion.

5. Acidification induced gel disruption

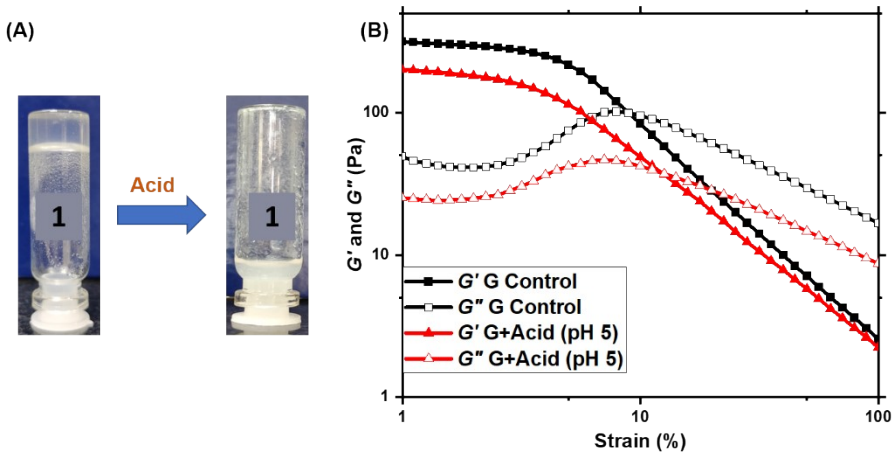

Figure S8. (A) Disruption of hydrogels of **1)** NapF-TREN (10 mg/mL) on acidification with 5 mM HCl (pH of the medium ~5). **(B)** Amplitude-sweep rheological profiles of NapF-TREN hydrogel at 10 rad/sec constant frequency and 25 °C, before and after acid addition. Colour code; Black-G Cntl (pristine gel), Red- Gel after acid addition.

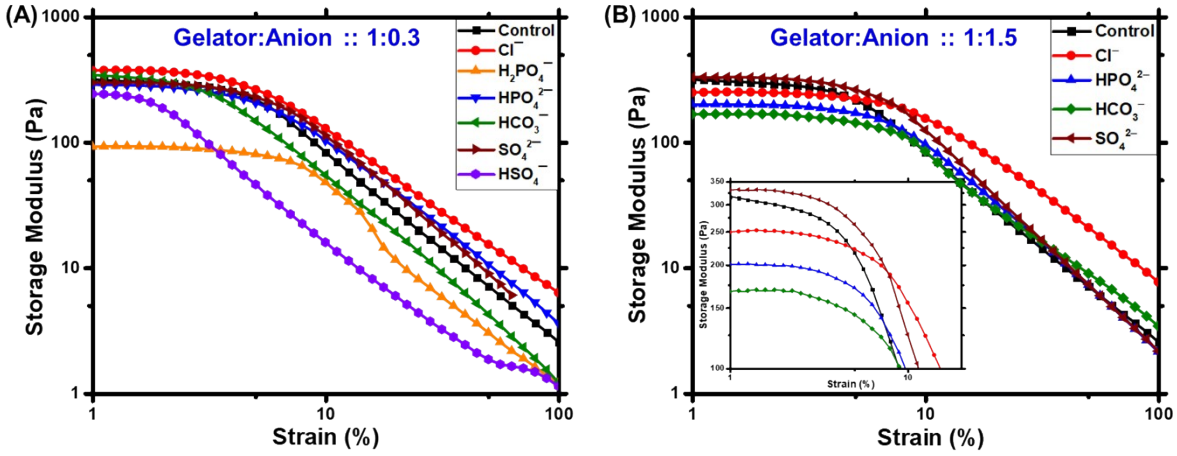

6. Rheology of hydrogels

Figure S9. Amplitude sweep rheological profiles of NapF-TREN (10 mg/mL, 22 mM) hydrogel in presence of different anions. **(A)** Upon addition of 0.3 equiv. (6.5 mM) anions, and **(B)** Upon addition of 1.5 equiv. (32 mM) of anions. The inset shows the zoomed region of 1-20% strain, highlighting the difference in the storage modulus values in presence of different anions. Colour code; Black-Control (pristine gel), Red-Cl^-, Orange-$H_2PO_4^-$ Gel, Blue-HPO_4^{2-}, Green-HCO_3^-, Wine-SO_4^{2-}, Violet-HSO_4^- Gel. The study was conducted at 298 K. 25 mm diameter cone plate was used at the top and a flat plate was used at the bottom for the strain sweep experiments.

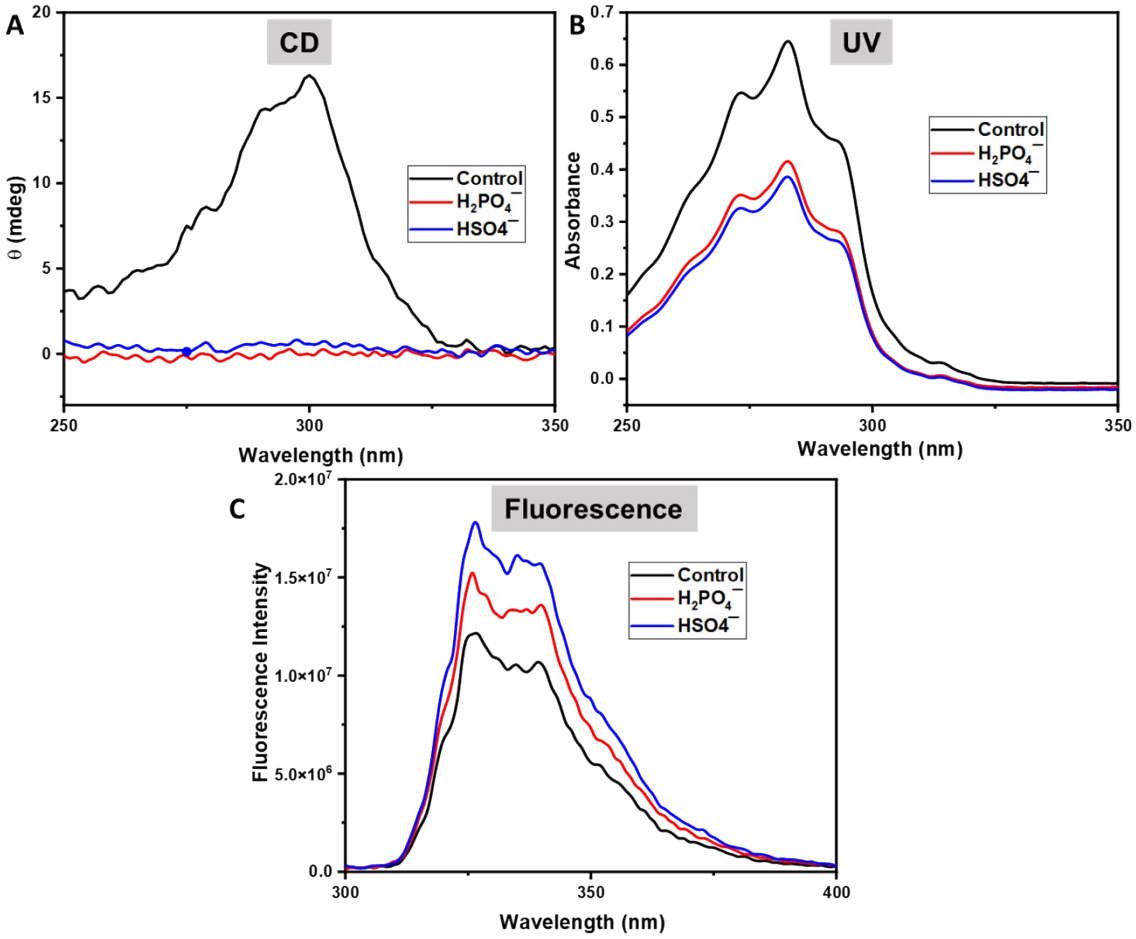

7. Spectroscopic study of NapF-TREN self-assembly with/without anions

Figure S10. Spectroscopy investigation of NapF-TREN self-assembly with/without presence of anions (3.3 mM, 1.5 equiv.). **A)** CD spectra (1 mg/mL, 2.2 mM), **B)** UV-Vis study (0.1 mg/mL, 0.22 mM) **C)** Fluorescence spectra (0.1 mg/mL, 0.22 mM). Black-Control sample (pristine self-assembly), Red-$H_2PO_4^-$ anion added self-assembly, and Blue-HSO_4^- anion added self-assembly. All experiments were performed in aqueous medium and the anion added as aqueous solution of the respective sodium salts.

8. TEM analysis of anion-induced changes

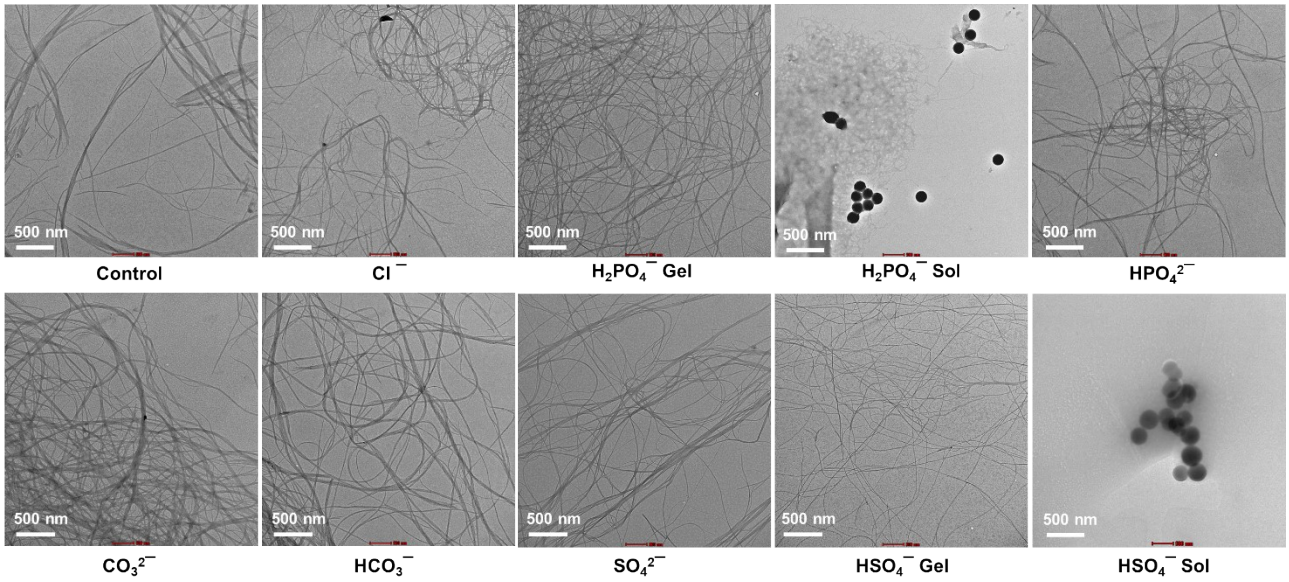

Figure S11. TEM images of NapF-TREN hydrogel (22 mM, Control) after the addition of different anions in sub-stoichiometric amounts (0.65 mM, 0.3 eqv. wrt the gelator). For $H_2PO_4^-$ and HSO_4^- anions, this induces partially disruption of the gel at the top side of the vial while intact gel remains at the bottom of the vial. Both the sol part and gel part were separately taken for recording TEM images. $H_2PO_4^-$ Gel/ HSO_4^- Gel refers the gel part of the partially disrupted hydrogel while $H_2PO_4^-$ Sol/ HSO_4^- Sol indicates the sol part of the hydrogel. Note the presence of nanospheres in the sol part and nanofibers in the gel part of samples treated with $H_2PO_4^-$ and HSO_4^- anions. Other anions did not affect the morphology of the self-assembly (or the macroscopic stability of the gels) considerably.

9. SEM analysis

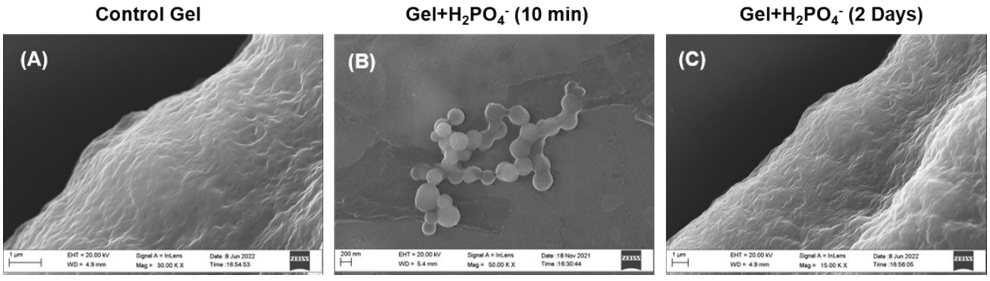

Figure S12. SEM images of **A)** NapF-TREN self-assemblies in water (Control Gel, c ≈ 2.2 mM) showing dense cloth-like morphology; and **B)** sample extracted 10 min after addition of $H_2PO_4^-$ anions (c ≈ 3.3 mM, 1.5 equiv.) showing nanoglobular morphology; **C)** sample obtained on ageing the NapF-TREN + $H_2PO_4^-$ for 2 days at RT.

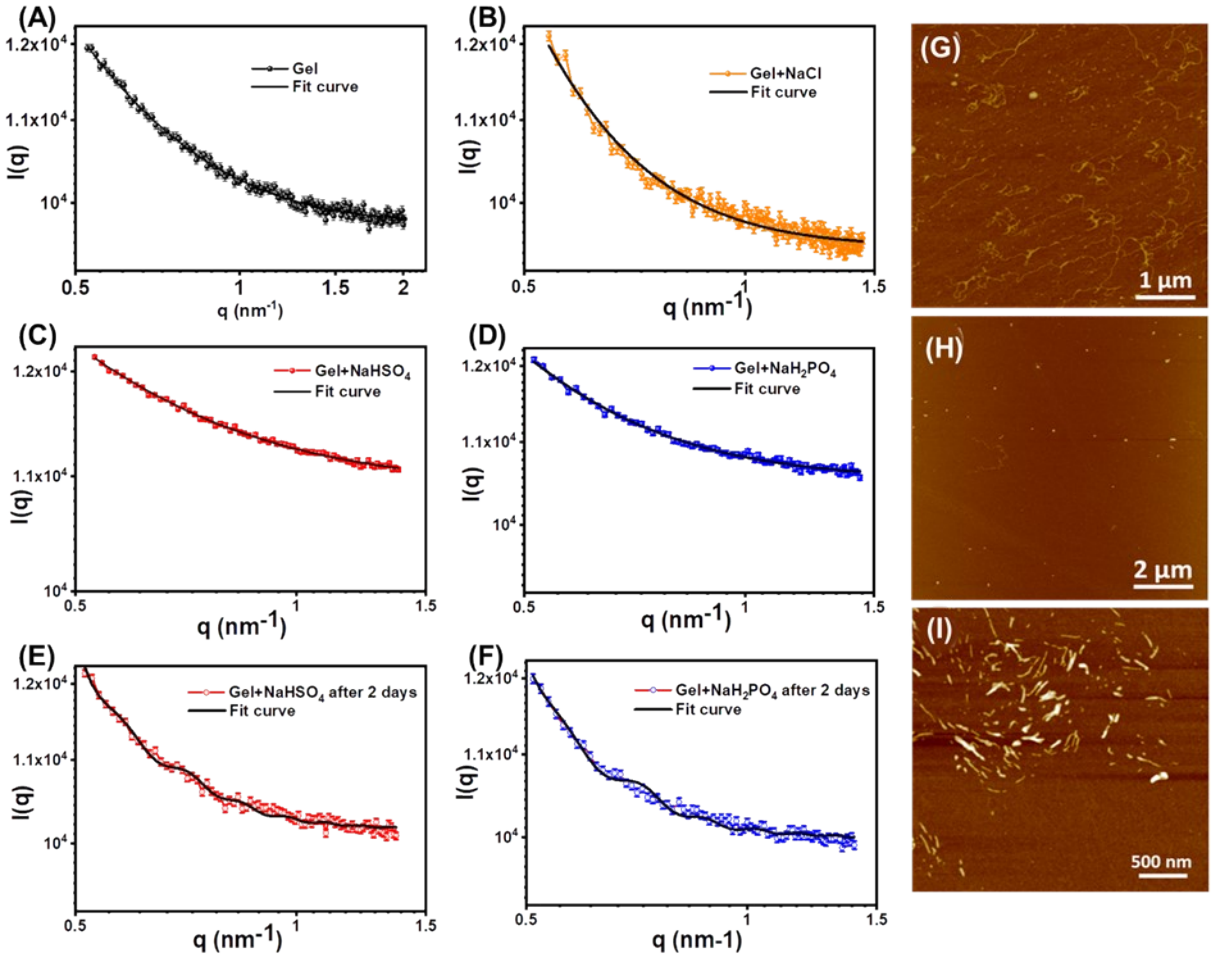

10. SAXS and AFM study of anion-effect on NapF-TREN self-assemblies

Figure S13. SAXS profiles and AFM studies on the effect of added anions (1.5 equivalent wrt. The gelator) on NapF-TREN self-assemblies (2.2 mM in water). **(A)** In absence of any added anion, and in presence of **(B)** NaCl, **(C)** $NaHSO_4$, **(D)** NaH_2PO_4, **(E)** $NaHSO_4$, after ageing the sample for 2 days at RT, and **(F)** NaH_2PO_4 after 2 days incubation at RT (25 °C). Solid lines are the fitting of the SAXS profiles (see Table S2 below). AFM images of **(G)** NapF-TREN + NaCl (indicates no change in nanofibrous morphology of the gels); **(H)** NapF-TREN + $NaHSO_4$ (result in transient nanoglobules), and **(I)** on ageing the NapF-TREN + $NaHSO_4$ sample for 2 days.

Table S2. Model and parameter for SAXS fitting**.**

Sample	Model fitted	R^2 value	Diameter of fiber or nanoparticles
NapF-TREN Self-assembly (Gelator)	Porod cylinder	1.13	15 nm
Gelator + NaCl	Porod cylinder	1.6	7.9 nm
Gelator+NaH_2PO_4	Sphere	1.08	7.3 nm
Gelator+$NaHSO_4$	Sphere	0.71	10 nm
Gelator + NaH_2PO_4 (after 2 days)	Porod cylinder	1.29	7 nm
Gelator+$NaHSO_4$ (after 2 days)	Porod cylinder	1.4	7.3 nm

11. NMR study

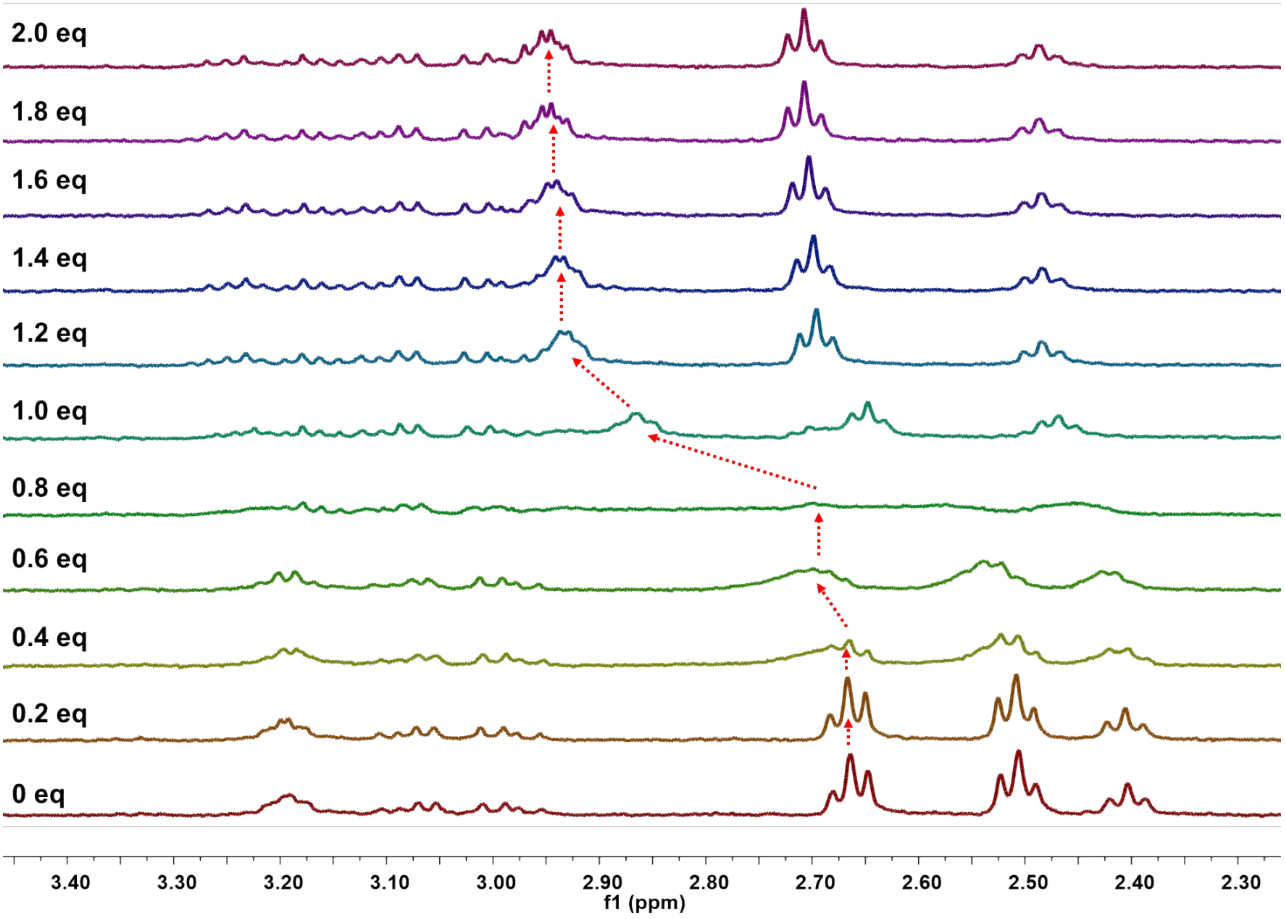

Figure S14. ^{1}H NMR (400 MHz, D_2O) titration of NapF-TREN (1 mg/mL, 2.2 mM) with $H_2PO_4^-$ anion. The titration proceeds from bottom to top. The bottom-most spectrum corresponds to the sample without added anion. The peak at 2.66 ppm corresponds to the NH_2 protons of the TREN-residues.

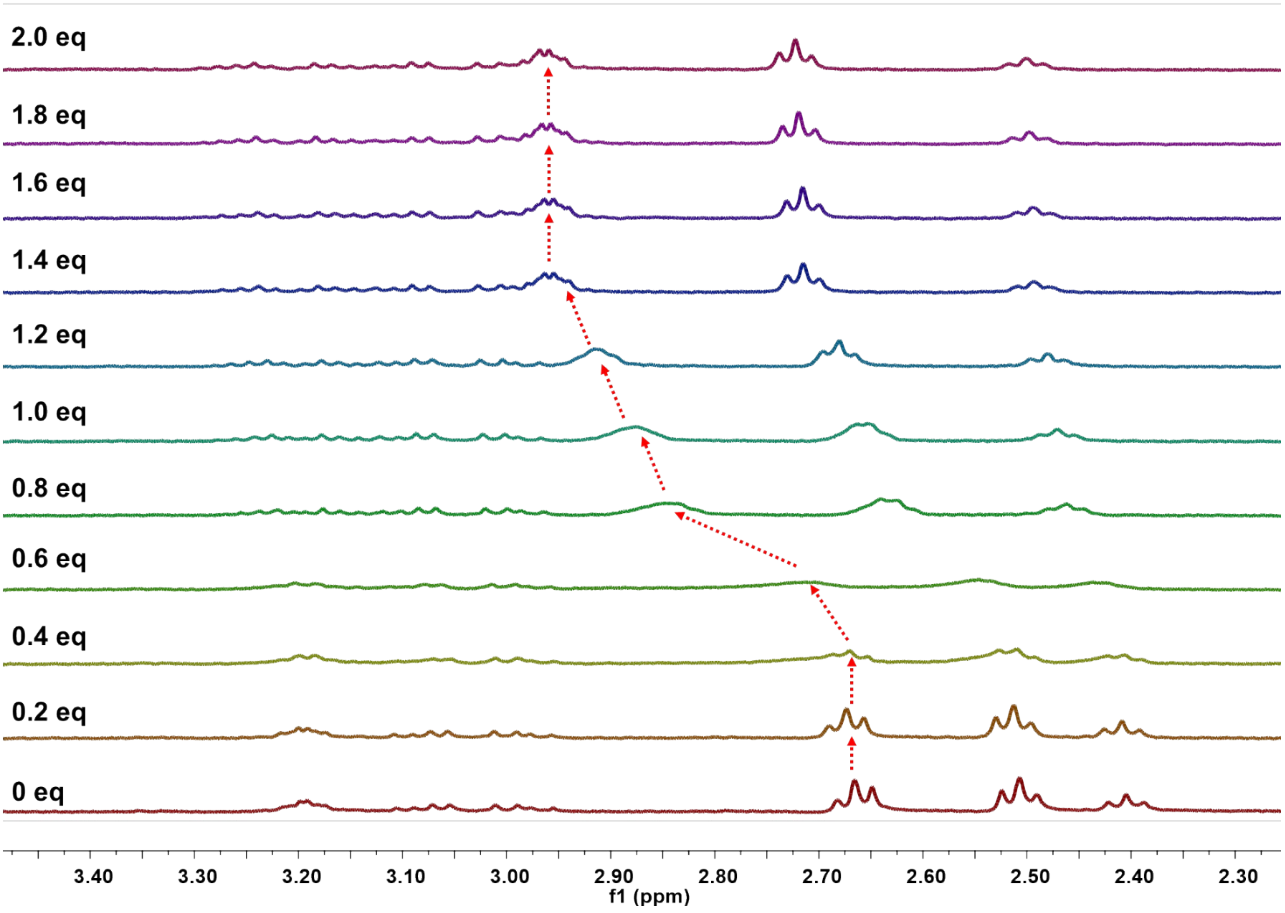

Figure S15. ^{1}H NMR (400 MHz, D_2O) titration of NapF-TREN (1 mg/mL, 2.2 mM) with HSO_4^- anion. The titration proceeds from bottom to top. The bottom-most spectrum corresponds to the sample without added anion. The peak at 2.66 ppm corresponds to the NH_2 protons of the TREN-residues.

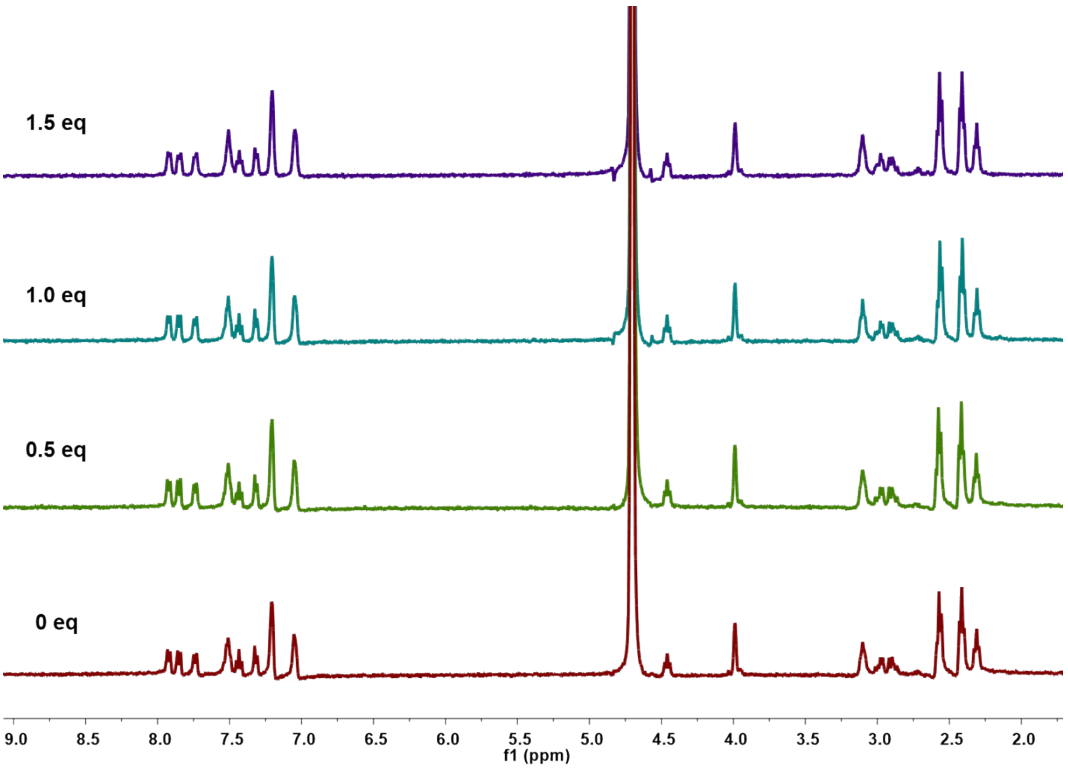

Figure S16. ^{1}H NMR (400 MHz, D_2O) titration of NapF-TREN (1 mg/mL, 2.2 mM) with HPO_4^{2-} anion. The titration proceeds from bottom to top. The bottom-most spectrum corresponds to the sample without added anion. The peak at 2.66 ppm corresponds to the NH_2 protons of the TREN-residues.

12. Drug release study

12.1 NapF-TREN-Dox adduct formation

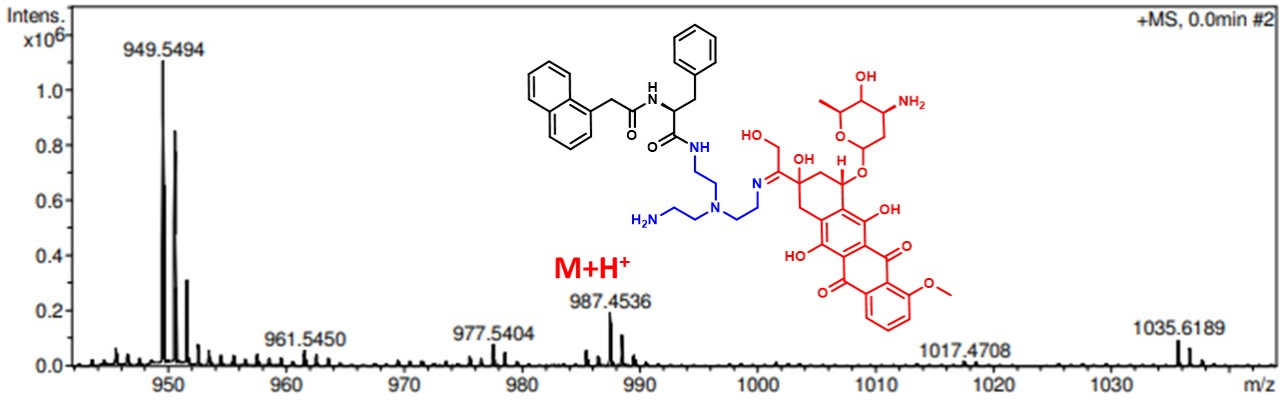

Figure S17. HRMS-ESI spectra showing formation of imine adduct between the gelator and doxorubicin. Peaks at 987, and 977, 961, 949 show the H^+, and fragmentation peaks with Na^+/ K^+ adducts of imine respectively.

12.2 UV-Vis study

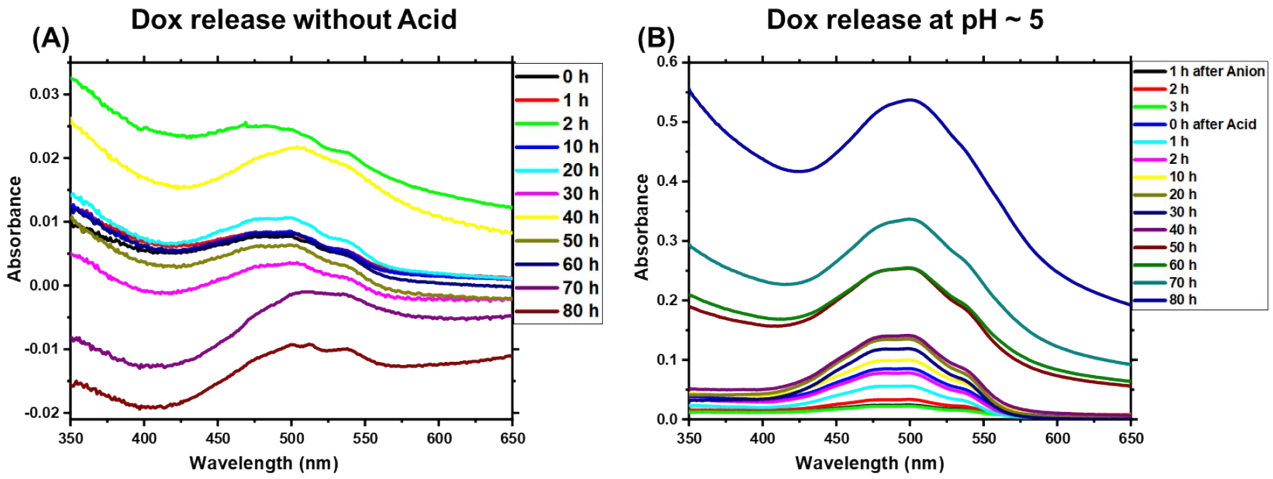

Figure S18. (A) UV-Vis spectroscopy study of Doxorubicin drug encapsulated NapF-TREN self-assembly without any anion and acid addition. **(B)** UV-Vis spectroscopy study of Doxorubicin drug encapsulated NapF-TREN self-assembly in the addition of $H_2PO_4^-$ anion and changing the pH sequentially at temperature 25 °C.

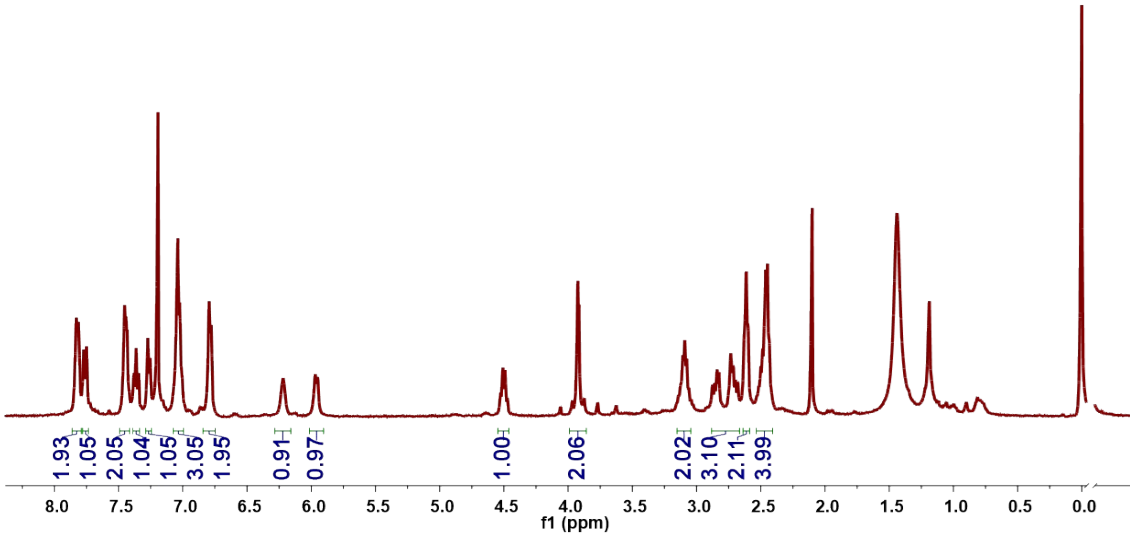

13. NMR and Mass data

Figure S19 (A). ^{1}H NMR of NapF-DETA (500 MHz, $CDCl_3$).

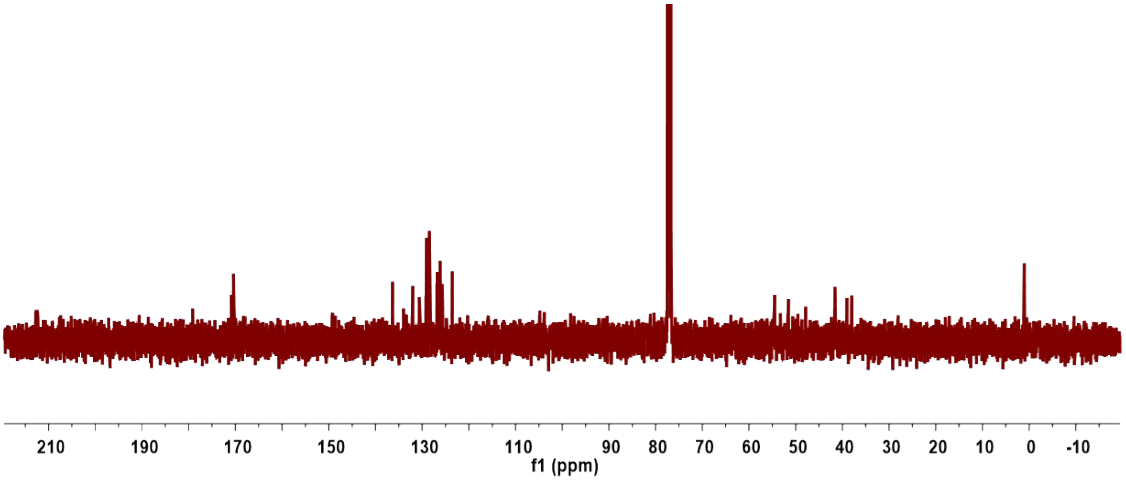

Figure S19 (B). ^{13}C NMR of NapF-DETA (125 MHz, $CDCl_3$).

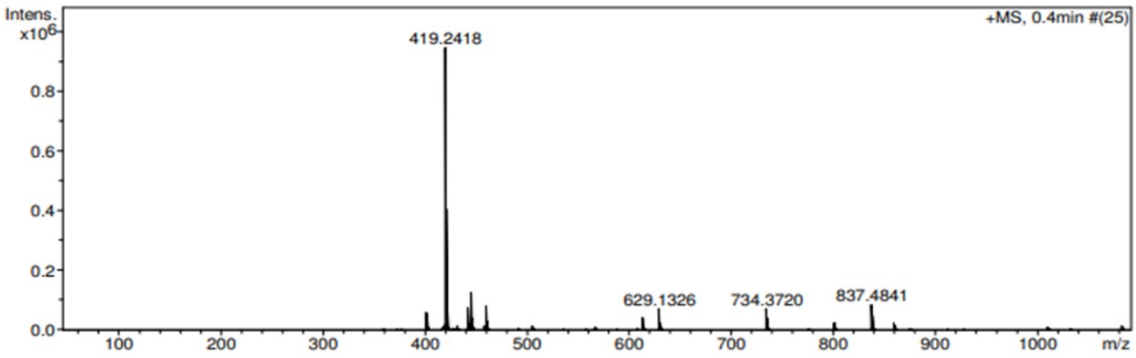

Figure S19 (C). HR-LCMS-ESI data of NapF-DETA.

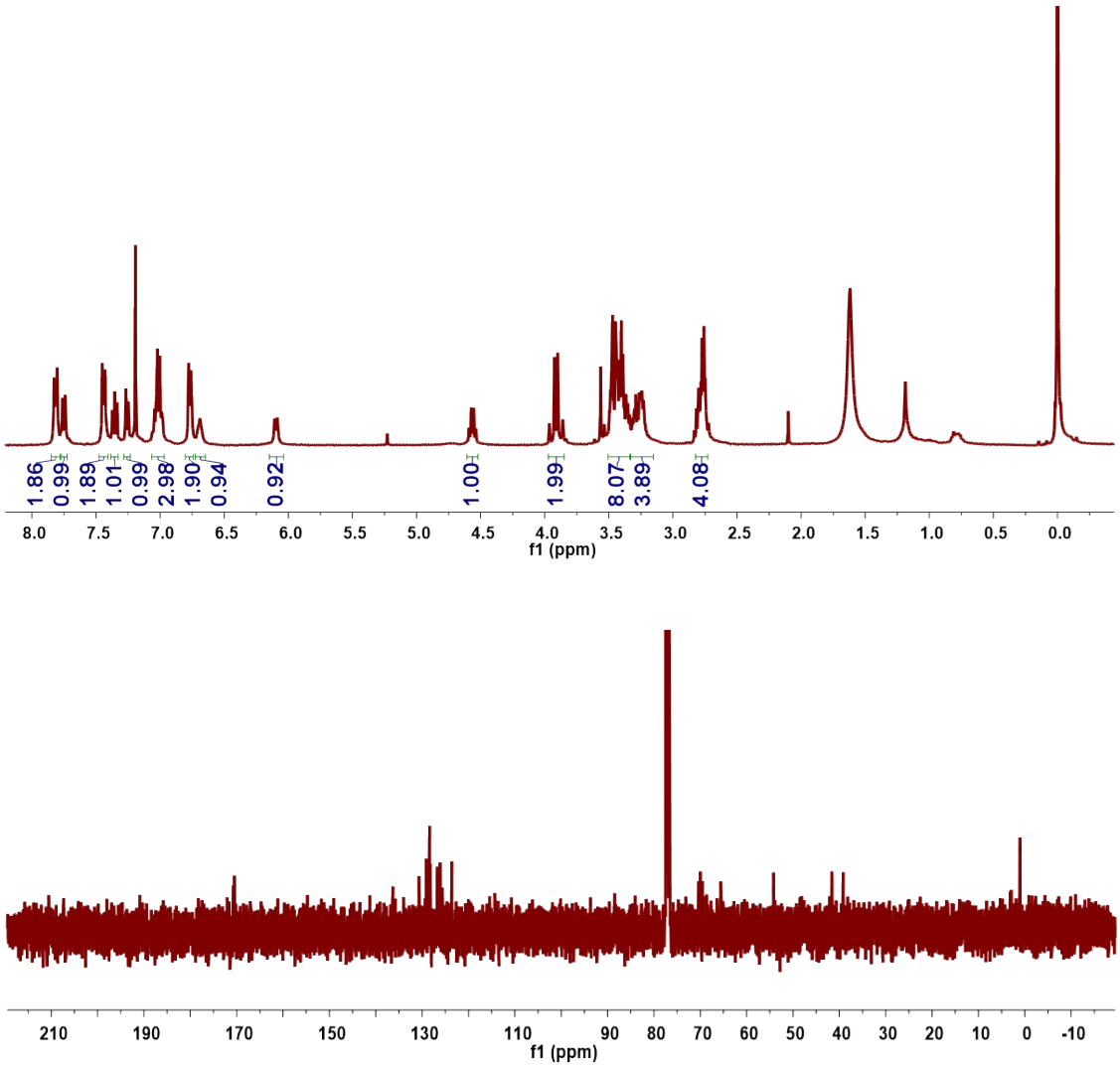

Figure S20 (A). ^{1}H NMR of NapF-EDEA (500 MHz, $CDCl_3$).

Figure S20 (B). ^{13}C NMR of NapF-EDEA (125 MHz, $CDCl_3$).

Figure S20 (C). HR-LCMS-ESI data of NapF-EDEA.

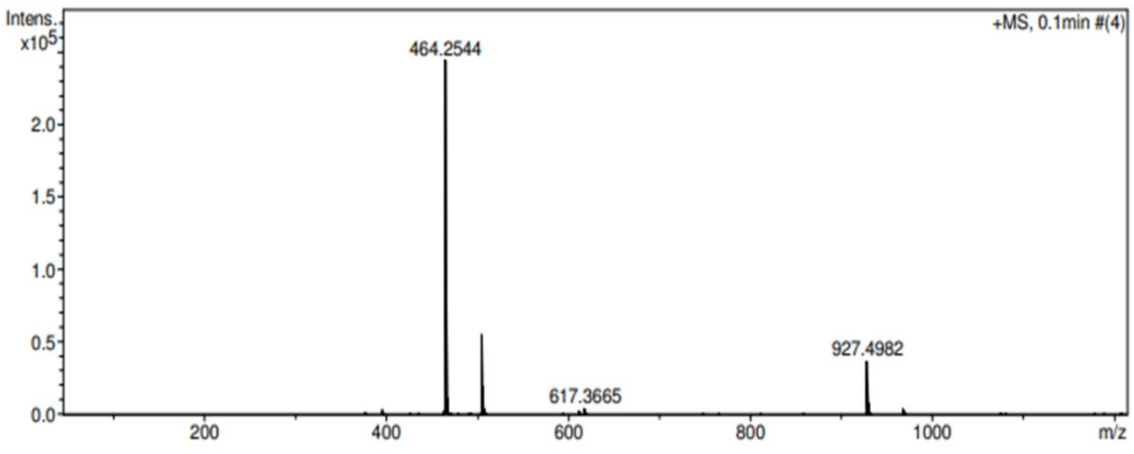

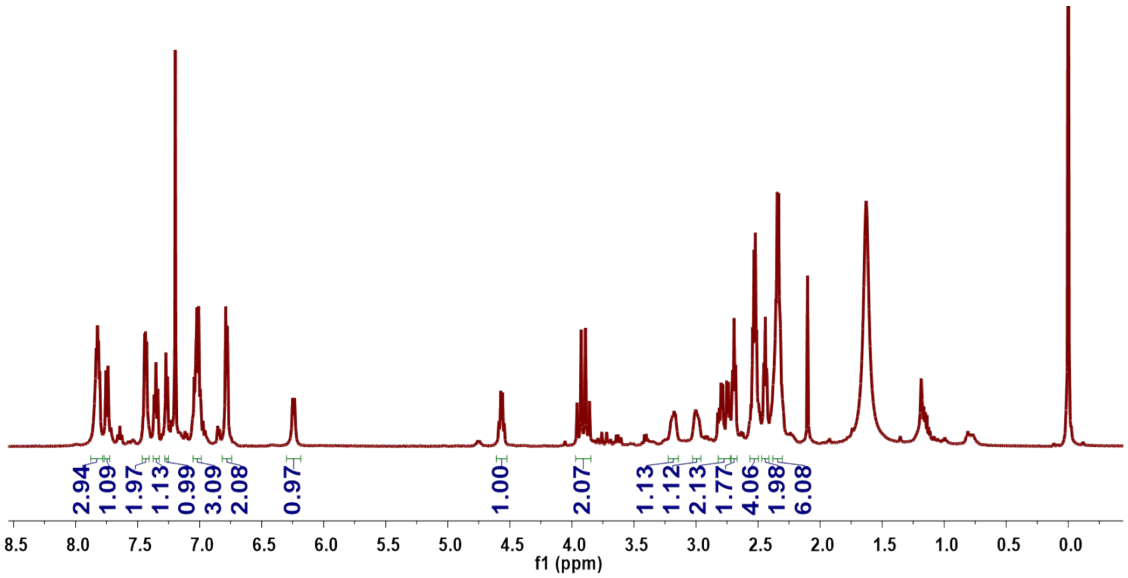

Figure S21 (A). ^{1}H NMR of NapF-TREN (500 MHz, $CDCl_3$).

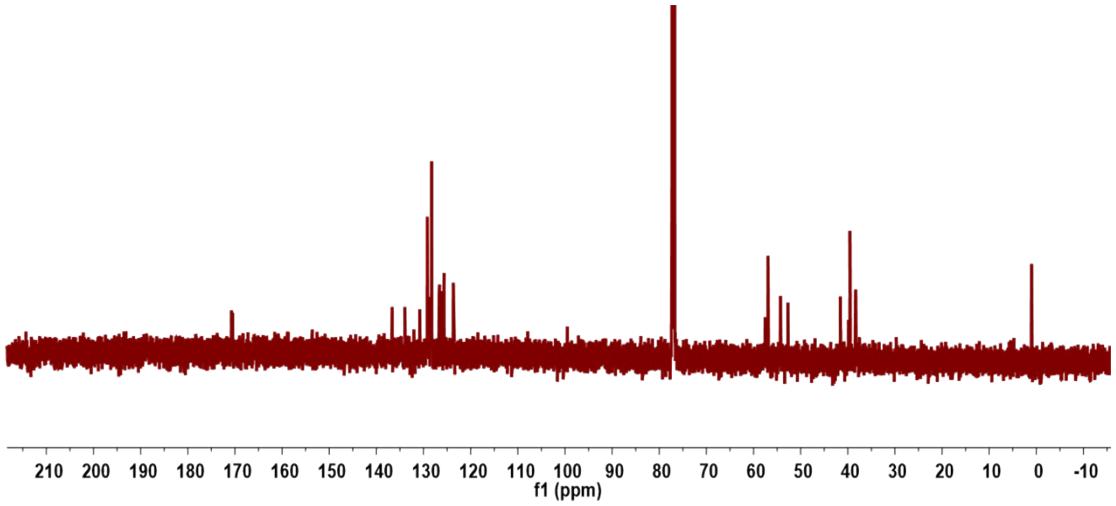

Figure S21 (B). ^{13}C NMR of NapF-TREN (125MHz, $CDCl_3$).

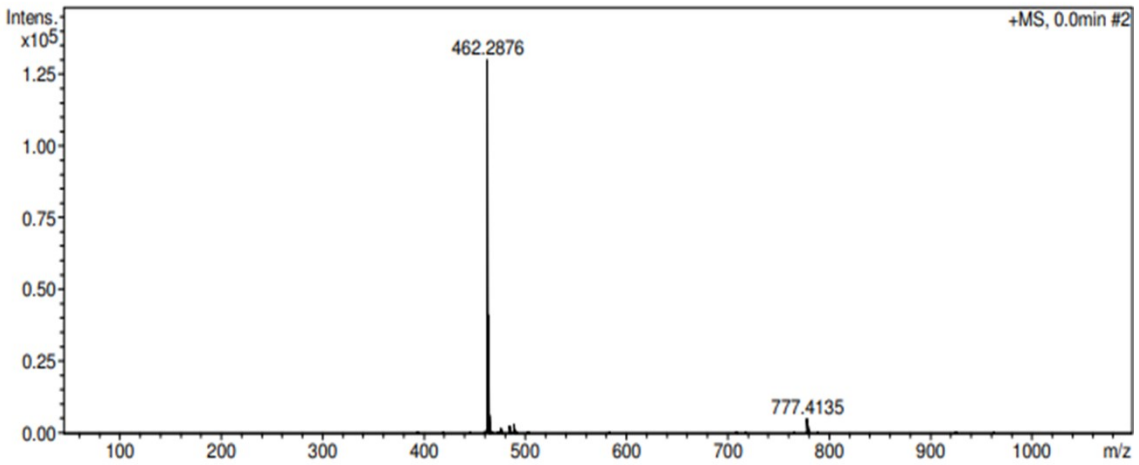

Figure S21 (C). HR-LCMS-ESI data of NapF-TREN.